

Transcriptome analysis of skeletal muscle in
dermatomyositis, polymyositis, and
dysferlinopathy, using a bioinformatics
approach

Ha-Neul Jeong

Department of Medicine

The Graduate School, Yonsei University

Transcriptome analysis of skeletal muscle in
dermatomyositis, polymyositis, and
dysferlinopathy, using a bioinformatics
approach

Directed by Professor Young-Chul Choi

The Doctoral Dissertation
submitted to the Department of Medicine,
the Graduate School of Yonsei University
in partial fulfillment of the requirements for the degree of
Doctor of Philosophy in Medical Science

Ha-Neul Jeong

June 2023

This certifies that the Doctoral Dissertation of
Ha-Neul Jeong is approved.

Thesis Supervisor: Young-Chul Choi

Thesis Committee Member#1: Hyung Jun Park

Thesis Committee Member#2: Seong Woong Kang

Thesis Committee Member#3: Young Yang

Thesis Committee Member#4: Seung-Hun Oh

The Graduate School
Yonsei University

June 2023

ACKNOWLEDGEMENTS

I am very pleased to finish my thesis. Throughout my years at graduate school in Yonsei university, I really learned a lot from this thesis work. I would like to thank my dissertation supervisor, Professor Young-Chul Choi, who has been a great mentor. I was able to complete this thesis thanks to his practical advice and encouragement. I also would like to thank Professors Hyung Jun Park, Seong Woong Kang, Young Yang, Seung-Hun Oh for their warm advice and feedback. Their varied perspectives have helped me to strengthen my work.

I also sincerely appreciate Researcher Taek-gyu Lee and Professor Seung-Tae Lee of the Department of Laboratory Medicine for their assistance in this study.

I would like to thank my parents and mother in law for their continuous love and support. Above all, I am grateful to my husband, Sang Hyeon An, who gives me endless love and encouragement, and my wonderful son, Jeong Woo, who makes my life shine. Lastly, I would like to say I love you to my precious daughter who will be born soon.

April, 2023
Ha-Neul Jeong

<TABLE OF CONTENTS>

ABSTRACT	iv
I. INTRODUCTION	1
II. MATERIALS AND METHODS	3
1. Participant enrollment	3
2. Clinical data collection	3
3. Ribonucleic acid (RNA) sequencing	3
4. Bioinformatics analysis	4
5. Ethics statement	5
III. RESULTS	6
1. Clinical data	6
2. Identification of DEGs	12
3. Enrichment analysis of DEGs	14
4. Identification of key modules and genes, using coexpression analysis	20
5. Identification of hub genes within important biological pathways in dysferlinopathy	23
6. Comparative analysis between PM and dysferlinopathy	26
IV. DISCUSSION	29
1. IFN1 signaling pathway in DM	29
2. Antigen processing and presentation of peptide antigen pathway in PM	31
3. Cellular response to stress in dysferlinopathy	31
A. <i>HSPA9</i>	32
B. Mammalian target of rapamycin complex 1 (mTORC1) pathway	33
4. DEGs downregulated in DM, PM, and dysferlinopathy	33
5. Comparative analysis between PM and dysferlinopathy	34
6. Limitations of this study	34
V. CONCLUSION	36

REFERENCES37
ABSTRACT(IN KOREAN)46

LIST OF FIGURES

Figure 1. PCA plot between each group of patients and the control	12
Figure 2. Heat maps of the DEGs of each patient group	13
Figure 3. Gene enrichment analysis of DEGs	16
Figure 4. Coexpression analysis of DEGs in DM	22
Figure 5. Coexpression analysis of DEGs in PM	23
Figure 6. Coexpression analysis of DEGs mapped to important pathways in dysferlinopathy	25
Figure 7. Comparative analysis between PM and dysferlinopathy	27

LIST OF TABLES

Table 1. Clinical features of patients with PM or DM	7
Table 2. Clinical features of patients with dysferlinopathy	10
Table 3. Upregulated DEGs involved in the interferon alpha/beta signaling pathway (R-HSA-909733) in DM	17
Table 4. Upregulated DEGs involved in the antigen processing and presentation of peptide antigen pathway (GO:0048002) in PM	19

ABSTRACT

Transcriptome analysis of skeletal muscle in dermatomyositis, polymyositis, and dysferlinopathy, using a bioinformatics approach

Ha-Neul Jeong

*Department of Medicine
The Graduate School, Yonsei University*

(Directed by Professor Young-Chul Choi)

Background: Polymyositis (PM) and dermatomyositis (DM) are distinct subgroups of idiopathic inflammatory myopathies. Dysferlinopathy, caused by a dysferlin gene mutation, usually presents in late adolescence with muscle weakness; the degenerative muscle changes are often accompanied by inflammatory infiltrates, frequently resulting in misdiagnosis as PM.

Objective: To identify differential biological pathways and hub genes related to PM, DM, and dysferlinopathy by using bioinformatics analysis, in order to understand their pathomechanisms and obtain guidance for therapy development.

Methods: We performed ribonucleic acid sequencing for vastus lateralis muscle biopsy samples from 7 patients with DM, 8 patients with PM, 8 patients with dysferlinopathy, and 5 control participants. Differentially expressed genes (DEGs) were identified using DESeq2. Enrichment analyses were performed to understand the functions and enriched pathways of DEGs. A protein–protein interaction (PPI) network was constructed, and gene clusters were identified using the molecular complex detection tool (MCODE) to identify hub genes.

Results: A total of 1048, 179, and 3807 DEGs were detected in DM, PM, and dysferlinopathy, respectively. Enrichment analyses revealed that upregulated DEGs were involved in the type 1 interferon signaling pathway in DM, antigen processing and peptide antigen presentation in PM, and the cellular response to stimuli in dysferlinopathy. The PPI

network and MCODE cluster identified 23 genes (*IFI6*, *IFI27*, *IFI35*, *IFIT1*, *IFIT2*, *IFIT3*, *IFIT5*, *IFITM1*, *IFITM3*, *IRF1*, *MX1*, *MX2*, *OAS1*, *OAS2*, *OAS3*, *HLA-A*, *HLA-B*, *HLA-C*, *STAT2*, *PSMB8*, *SAMHD1*, *XAF1*, and *RSAD2*) related to the type 1 interferon signaling pathway in DM, 4 genes (*PDIA3*, *HLA-C*, *B2M*, and *TAP1*) related to major histocompatibility complex class I formation and quality control in PM, and 7 genes (*HSPA9*, *RPTOR*, *MTOR*, *LAMTOR1*, *LAMTOR5*, *ATP6V0D1*, and *ATP6V0B*) related to the cellular response to stress in dysferlinopathy.

Conclusion: Intramuscular transcriptome analysis using a bioinformatics approach identified overexpression of genes related to the IFN1 signaling pathway in DM and overexpression of genes related to MHC-I formation and quality control in PM. In dysferlinopathy, overexpression of *HSPA9* and the mammalian target of rapamycin (mTOR) complex 1 signaling pathway genes was detected. These results may provide new directions for future research on their pathogenesis and treatment.

Key words : dermatomyositis, polymyositis, dysferlinopathy, transcriptome analysis, ribonucleic acid sequencing, bioinformatics analysis

Transcriptome analysis of skeletal muscle in dermatomyositis, polymyositis, and dysferlinopathy, using a bioinformatics approach

Ha-Neul Jeong

*Department of Medicine
The Graduate School, Yonsei University*

(Directed by Professor Young-Chul Choi)

I. INTRODUCTION

Idiopathic inflammatory myopathies (IIMs) comprise a heterogeneous group of autoimmune conditions characterized by skeletal muscle weakness and inflammation. The main clinical subtypes of IIM are classified as follows: dermatomyositis (DM); polymyositis (PM); immune-mediated necrotizing myopathy (IMNM); overlap syndrome with myositis (overlap myositis [OM]), including anti-synthetase syndrome (ASS); and inclusion body myositis (IBM).¹ The pathogenic mechanisms underlying the different myositis types and subtypes remain unclear. In recent years, different approaches, including genomic, epigenetic, transcriptomic, proteomic, and autoantibody studies, have been used to understand IIM pathogenesis.²

Studies involving expression profiling of patients with DM or PM showed that the genes related to major histocompatibility complex (MHC) class I (MHC-I), MHC class II (MHC-II), cytokines, adhesion molecules, the actin cytoskeleton, and immunoglobulins were differentially expressed in muscle tissue.^{3,4} In particular, the type 1 interferon (IFN1) pathway is relevant to DM pathogenesis.⁵ Overexpression of IFN1-inducible genes has been detected in the muscle, peripheral blood, and skin of patients with DM.⁵⁻⁸ PM is generally considered a prototypic T cell-mediated autoimmune myopathy.⁹

Dysferlinopathy, caused by a dysferlin gene mutation, usually presents in late

adolescence with muscle weakness; the degenerative muscle changes are often accompanied by inflammatory infiltrates, resulting in misdiagnosis as PM.¹⁰ Dysferlin protein appears to play a role in calcium-dependent vesicle-mediated muscle membrane repair.¹¹ Furthermore, it is proposed to play diverse roles in cell adhesion, angiogenesis, and myogenesis.^{12,13} The precise pathogenic mechanism underlying dysferlinopathy remains unclear; it is hypothesized that defective membrane repair in dysferlin-deficient muscle leads to muscular dystrophy associated with remarkable muscle inflammation.¹⁴ Previous research has shown that the inflammasome pathway components are upregulated and activated in the muscles of patients and mice with dysferlinopathy.¹⁵ Dysferlin-deficient muscles also exhibit ubiquitin–proteasomal pathway activation, complement system factor upregulation, and macrophage infiltration.¹⁶⁻¹⁸

Ribonucleic acid sequencing (RNA-Seq) helps detect and quantify complementary deoxyribonucleic acid (cDNA) via next-generation sequencing. It provides comprehensive understanding of alternative gene spliced transcripts, posttranscriptional modifications, gene fusion, single-nucleotide variations, and gene expression changes.¹⁹ In recent years, bioinformatics analysis of gene expression profiles has played a critical role in studying human disease pathogenesis. Differences in the gene expression levels of disease and healthy groups can help detect cellular changes related to disease status, thereby suggesting pathomechanisms.²⁰

In this study, we aimed to understand the transcriptomic signature and pathomechanism of DM, PM, and dysferlinopathy. We generated transcriptome profiles of muscles from patients with DM, PM, or dysferlinopathy and analyzed their gene expression profiles by using bioinformatics. Additionally, we compared the transcriptome profiles of dysferlinopathy and PM to help identify potential biomarker genes for differentiating between these two clinically similar myopathies because dysferlinopathy is often misdiagnosed as PM.

II. MATERIALS AND METHODS

1. Participant enrollment

We reviewed the medical records from January 2002 to October 2016 in the myopathy database of Gangnam Severance Hospital. The study included 7, 8, 8, and 5 vastus lateralis muscle biopsy samples from 7 patients with DM, 8 patients with PM, 8 patients with dysferlinopathy, and 5 control participants, respectively. The 15 patients with DM or PM had been diagnosed on the basis of the 2017 European League Against Rheumatism/American College of Rheumatology classification criteria for adult and juvenile IIMs,²¹ by combining the data on clinical characteristics and serological, electrophysiological, and histological evaluations of skeletal muscle biopsies. The diagnosis of dysferlinopathy in the 8 patients had been genetically confirmed. We selected 5 control participants who fulfilled the following criteria: (i) normal muscle pathological features, (ii) normal serum creatine kinase (CK) level, (iii) absence of definite muscle weakness, and (iv) availability of vastus lateralis muscle biopsy samples.

2. Clinical data collection

Clinical records of all the participants were reviewed to obtain the following information: age at diagnosis, age at onset of symptoms, pattern of weakness on clinical examination, serum CK levels, electrophysiological results, and findings from muscle pathology analysis.

3. Ribonucleic acid (RNA) sequencing

cDNA libraries were constructed using the TruSeq RNA library kit, with 1 μ g total RNA. The protocol consisted of the following steps: polyA-selected RNA extraction, RNA fragmentation, random hexamer-primed reverse transcription, and 100-nt paired-end sequencing performed using the Illumina HiSeq2500 system. The libraries were quantified using quantitative polymerase chain reaction (qPCR) performed according to

the qPCR Quantification Protocol Guide and qualified using an Agilent Technologies 2100 Bioanalyzer. The sequencer reads were processed and then aligned to the hg19 reference genome by using the STAR v2.7.10a algorithm to perform the alignment.²² STAR is an algorithm for aligning high-throughput short RNA-Seq data to a reference genome; it was developed to overcome the speed and accuracy issue. The reference genome and annotation data were downloaded from the UCSC Table Browser (<http://genome.ucsc.edu>).

For gene annotation, the gencode version 19 annotation file was downloaded from GENCODE (<https://www.gencodegenes.org>). While running the STAR alignment, “--quantMode” was enabled to create a gene count file. Appropriate read counts were selected on the basis of the sequencing protocol. These raw reads were deposited in the NCBI Sequence Read Archive (SRA) database (accession number: SRP149027).

4. Bioinformatics analysis

Adaptors were removed from the raw reads by using trim-galore (0.6.6). After the adaptors were trimmed, alignment was performed using an inhouse STAR alignment pipeline by following the recommended procedures.²² The GENCODE version 19 annotation database was used to annotate genes. Read counts, which were obtained from the STAR alignment results, were normalized to compare expression levels between samples by using the DESeq2 package. In addition, DESeq2 identified differentially expressed genes (DEGs). The criteria for identifying DEGs were false discovery rate (FDR) < 0.05 and log₂ fold change ≥ 2 or ≤ -2 . Principal component analysis (PCA) was performed to confirm how gene expression in each sample was characterized by pathogenic features. The overall expression pattern in each comparison group was observed using a gene expression heat map.

Gene enrichment analysis of DEGs was performed using Metascape (<http://metascape.org>), which includes gene ontology (GO) processes,²³ Kyoto Encyclopedia of Genes and Genomes (KEGG) signaling pathways,²⁴ and reactome

pathways.²⁵ Postprocessing of data generated via Metascape analysis involved analysis of Kappa similarities among all pairs of enriched terms and resulted in the absorption of most redundancies into representative clusters. The results extract representative processes from the reporting of multiple ontologies.²⁶ For coexpression analysis, the protein–protein interaction (PPI) network was constructed using the Metascape website; the results were further visualized using the Cytoscape software (version 3.9.1).²⁷ Next, molecular complex detection tool (MCODE) (version 1.5.1)²⁸ was utilized to identify the most important modules in the PPI network. The cutoff values were set as follows: node score cutoff = 0.2, maximal depth = 100, K-Core = 2, and degree cutoff = 2. Significant genes were detected using MCODE analysis.

5. Ethics statement

The institutional review board of Gangnam Severance Hospital, South Korea, approved the research protocol (IRB No. 3-2021-0450). All participants provided informed consent for clinical data collection and genetic analysis.

III. RESULTS

1. Clinical data

Clinical data review for a total of 15 patients with PM or DM confirmed that the diagnosis was acceptable according to the 2017 European League Against Rheumatism/American College of Rheumatology classification criteria.²¹ The clinical features of the patients with PM or DM have been provided in Table 1.

The clinical features of the 8 patients with dysferlinopathy were as follows: miyoshi distal myopathy (3 patients), limb-girdle muscular dystrophy (3 patients), proximodistal type (1 patient), and hyperCKemia (1 patient). Immunohistochemical analysis of dysferlin showed total loss of expression in 7 patients and decreased expression in 1 patient. Two patients with dysferlinopathy had a history of initial misdiagnosis as PM. The clinical features of the patients with dysferlinopathy have been provided in Table 2.

The control group consisted of 2 men and 3 women, with ages ranging from 28 to 47 years. Two patients had been diagnosed with cramps, and three patients had been diagnosed with psychogenic weakness (1 patient), psychogenic dystonia (1 patient), and myalgia (1 patient).

Table 1. Clinical features of patients with PM or DM.

Case	Sex	Age (years)	Onset	Clinical feature	CK (U/L)	EMG results	Pathologic findings
PM1	F	35	1MA	Symmetric proximal weakness	3283	N/A	Myopathic changes
PM2	F	35	2MA	Symmetric proximal weakness	5670	Myopathic	Endomysial inflammatory cell infiltration
PM3	F	49	1MA	Symmetric proximal weakness	15,216	Myopathic	Endomysial inflammatory cell infiltration
PM4	M	48	7YA	Symmetric proximal weakness	1877	Myopathic	Endomysial inflammatory cell infiltration
PM5	F	21	1YA	Symmetric proximal weakness	2090	Myopathic	Perivascular inflammatory cell infiltration
PM6	F	46	3YA	Symmetric proximal weakness	321	Myopathic	Endomysial inflammatory cell infiltration

PM7	F	48	1MA	Symmetric proximal weakness	13,940	Myopathic	Endomysial inflammatory cell infiltration
PM8	F	25	7MA	Symmetric proximal weakness	12,180	Myopathic	Endomysial inflammatory cell infiltration
DM1	F	38	1YA	Skin lesion* and symmetric proximal weakness	75	Myopathic	Perifascicular atrophy and inflammatory cell infiltration
DM2	F	29	2MA	Skin lesion* and symmetric proximal weakness	584	N/A	Perifascicular atrophy and inflammatory cell infiltration
DM3	F	22	9MA	Skin lesion* and symmetric proximal weakness	2599	Myopathic	Perifascicular atrophy and inflammatory cell infiltration
DM4	F	27	1YA	Skin lesion* and symmetric proximal weakness	1178	Myopathic	Perifascicular atrophy and inflammatory cell infiltration

DM5	F	40	4MA	Skin lesion* and symmetric proximal weakness	285	Myopathic	Perifascicular atrophy and inflammatory cell infiltration
DM6	F	42	4MA	Skin lesion* and symmetric proximal weakness	631	Myopathic	Perifascicular atrophy and inflammatory cell infiltration
DM7	M	40	3MA	Skin lesion* and symmetric proximal weakness	13712	N/A	Inflammatory cell infiltration

Abbreviations: PM, polymyositis; DM, dermatomyositis; MA, months ago; YA, years ago; CK, creatine kinase; EMG, electromyography; N/A: not available

* Skin lesions included rash typical of DM (heliotrope rash, Gottron's papules, Gottron's sign).

Table 2. Clinical features of patients with dysferlinopathy.

Case	Sex	Age	Onset	Clinical features	Dysferlin expression	Inflammatory cell infiltration	Likely/pathogenic variant
DYS1	F	39	2YA	Miyoshi distal myopathy	Total loss	+	c.663+1G>C/c.4886+1249G>T
DYS2	F	40	14YA	Miyoshi distal myopathy	Total loss	-	c.2974T>C/c.2997G>T
DYS3	F	37	3YA	Limb-girdle muscular dystrophy	Total loss	+	c.3032-1G>A/c.3032-1G>A
DYS4	M	38	21YA	Proximodistal type	Total loss	-	c.1284+2T>C/c.2494C>T
DYS5	F	26	5YA	Limb-girdle muscular dystrophy	Total loss	+	c.663+1G>C/c.937+1G>A
DYS6	F	31	1YA	HyperCKemia	Total loss	-	c.3407delG/c.2633_2634delTT
DYS7	F	36	5YA	Limb-girdle muscular	Total loss	+	c.1363_1364delAT/c.757C>T

dystrophy							
DYS8	M	40	10YA	Miyoshi distal myopathy	Decreased expression	-	c.1284+2T>C/c.2997G>T

Abbreviations: DYS, dysferlinopathy; MA, months ago; YA, years ago

2. Identification of DEGs

Bioinformatics analysis showed the presence of DEGs in all patient groups. PCA showed differences between the patient and control samples (Figure 1). Patients with DM could be clearly distinguished from those in the control group. Patients with dysferlinopathy were also observed as a distinct group, except for 1 patient (DYS8). In contrast, patients with PM could not be obviously distinguished from controls. The number of DEGs obtained in the analysis was 1048, 179, and 3807 for DM, PM, and dysferlinopathy, respectively (Figure 2).

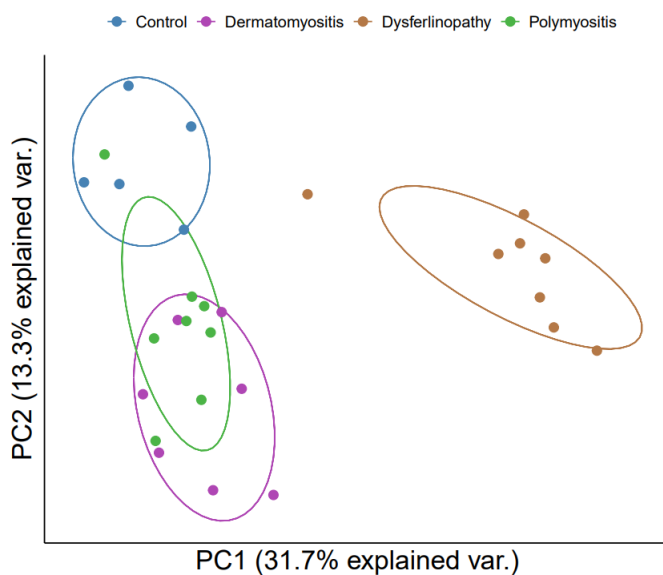
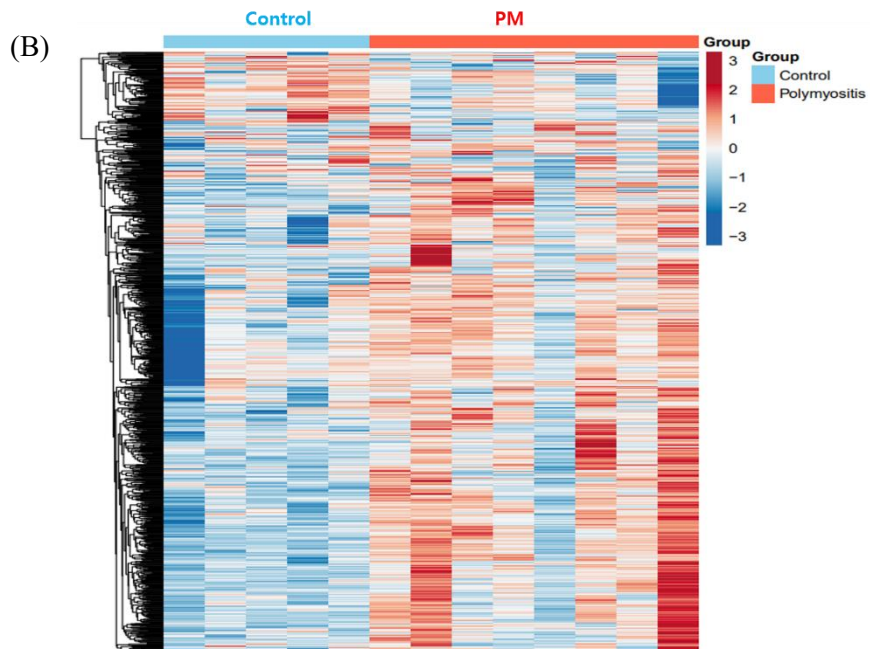
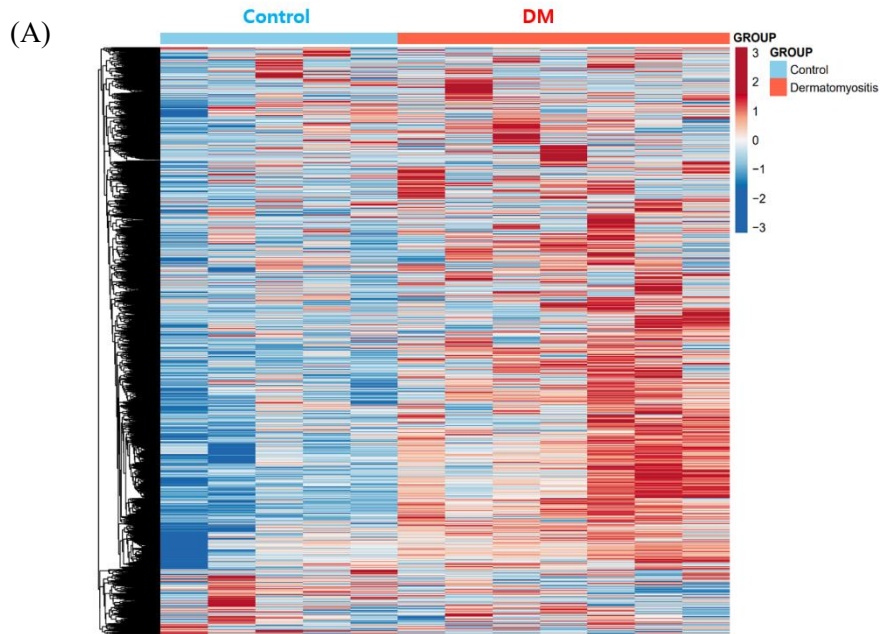


Figure 1. PCA plot between each group of patients and the control. PCA visualized DM and dysferlinopathy as groups distinct from the control. The distinction between PM and the control was ambiguous.

Abbreviations: var., variance



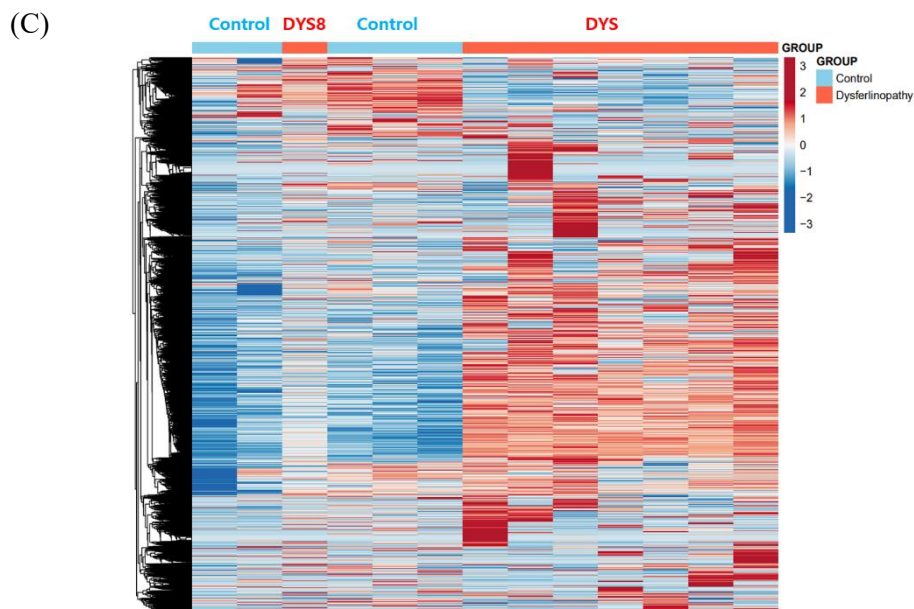


Figure 2. Heat maps of the DEGs of each patient group. (A) Heat map of the genes differentially expressed between DM and the control. (B) Heat map of the genes differentially expressed between PM and the control. (C) Heat map of the genes differentially expressed between dysferlinopathy and the control.

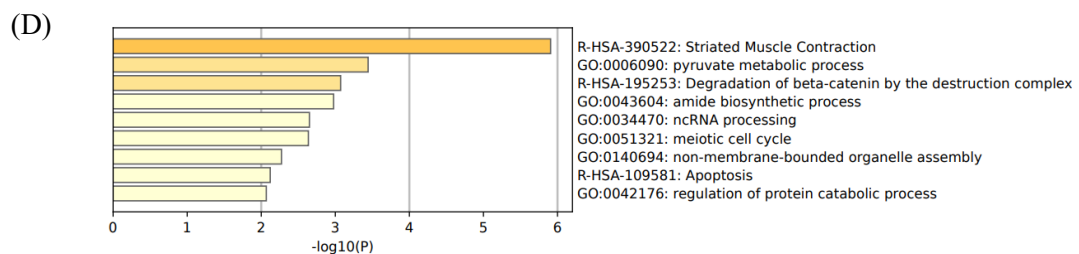
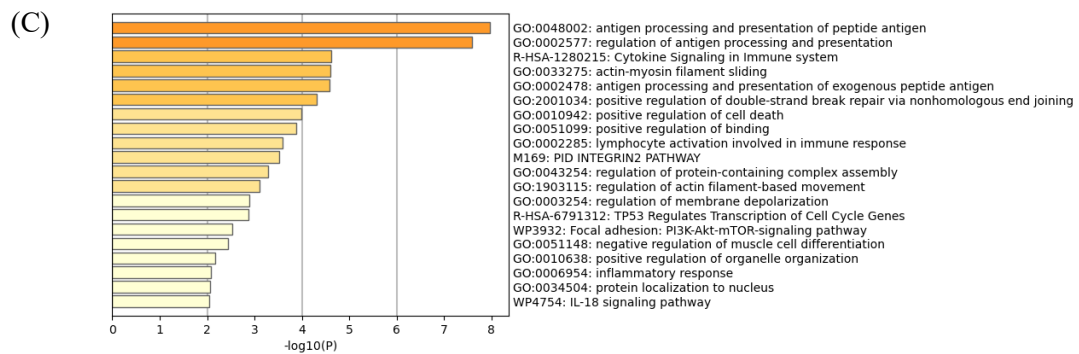
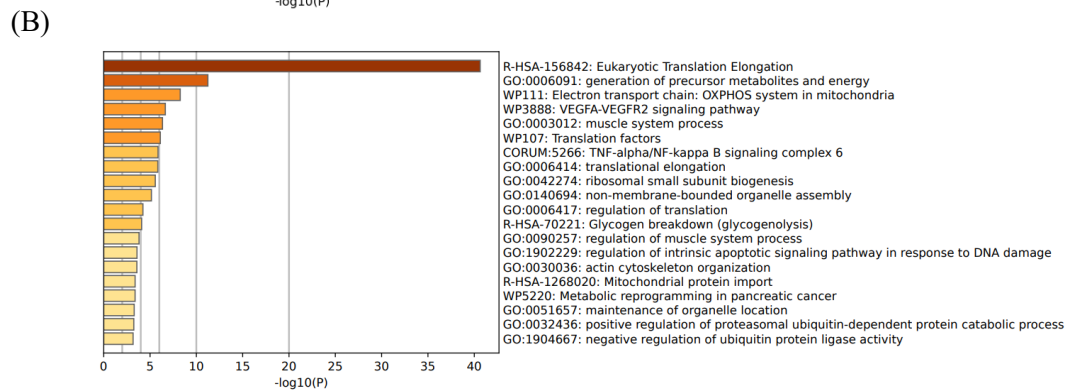
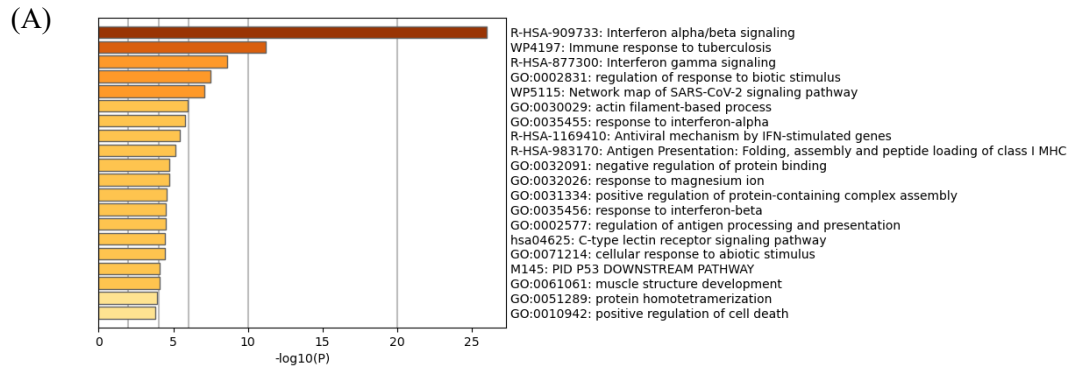
3. Enrichment analysis of DEGs

The DEGs were categorized by gene enrichment analysis, and the top 10 biological pathways of upregulated and downregulated DEGs in patients with DM, PM, or dysferlinopathy have been provided in Figure 3. The results revealed that 576 DEGs were upregulated in DM and were most abundant in the interferon alpha/beta signaling pathway (R-HSA-909733). Twenty-six DEGs mapped to that reactome pathway: *IFI6*, *IFI27*, *IFI35*, *IFIT1*, *IFIT2*, *IFIT3*, *IFIT5*, *IFITM1*, *IFITM3*, *IRF1*, *MX1*, *MX2*, *OAS1*, *OAS2*, *OAS3*, *HLA-A*, *HLA-B*, *HLA-C*, *STAT2*, *ISG15*, *PSMB8*, *SOCS3*, *USP18*,

SAMHD1, *XAF1*, and *RSAD2*. Additional information regarding these genes is provided in Table 3. The findings showed that 472 DEGs were downregulated in DM; these genes were most abundant in the eukaryotic translation elongation pathway (R-HSA-156842). In addition, 110 DEGs mapped to that reactome pathway.

In the case of PM, 112 DEGs were upregulated and were most abundant in the antigen processing and presentation of peptide antigen pathway (GO:0048002); 24 DEGs mapped to that GO pathway: *B2M*, *CD74*, *PDIA3*, *HLA-C*, *HLA-DRA*, *TAP1*, *TAPBPL*, *CDKN1A*, *GADD45A*, *ITGAL*, *PSMD1*, *ICAM2*, *KIF22*, *SPTBN2*, *TNFRSF14*, *SOCS3*, *DTX3L*, *RHOC*, *ZNF627*, *CREB3L2*, *IFIT3*, *PLAU*, *GSDMD*, and *TBC1D10C*. Additional information regarding these genes has been provided in Table 4. Sixty-seven DEGs were downregulated in PM; these genes were most abundant in the striated muscle contraction pathway (R-HSA-390522). Six DEGs (*MYBPC2*, *TNNC2*, *TNNI2*, *TNNT3*, *SCN9A*, and *MYH1*) mapped to that reactome pathway.

In the case of dysferlinopathy, 1650 DEGs were upregulated; these genes were most abundant in the cellular response to stimuli (R-HSA-8953897). Furthermore, 261 DEGs were mapped to that reactome pathway. The other top-ranked biological pathways were as follows: VEGFA-VEGFR2 signaling pathway (WP3888), actin filament-based process (GO:0030029), muscle structure development (GO:0061061), pathway of neurodegeneration – multiple diseases (hsa05022), and vesicle-mediated transport (R-HSA-5653656). Furthermore, 2157 DEGs were downregulated in dysferlinopathy; these genes were most abundant in the DNA metabolic process pathway (GO:0006259). Sixty-two DEGs were mapped to that GO pathway. The other top-ranked biological pathways were as follows: protein localization to organelle (GO:0033365), regulation of response to DNA damage stimulus (GO:2001020), cell cycle (R-HSA-1640170), organelle assembly (GO:0070925), and cellular amide metabolic process (GO:0043603).



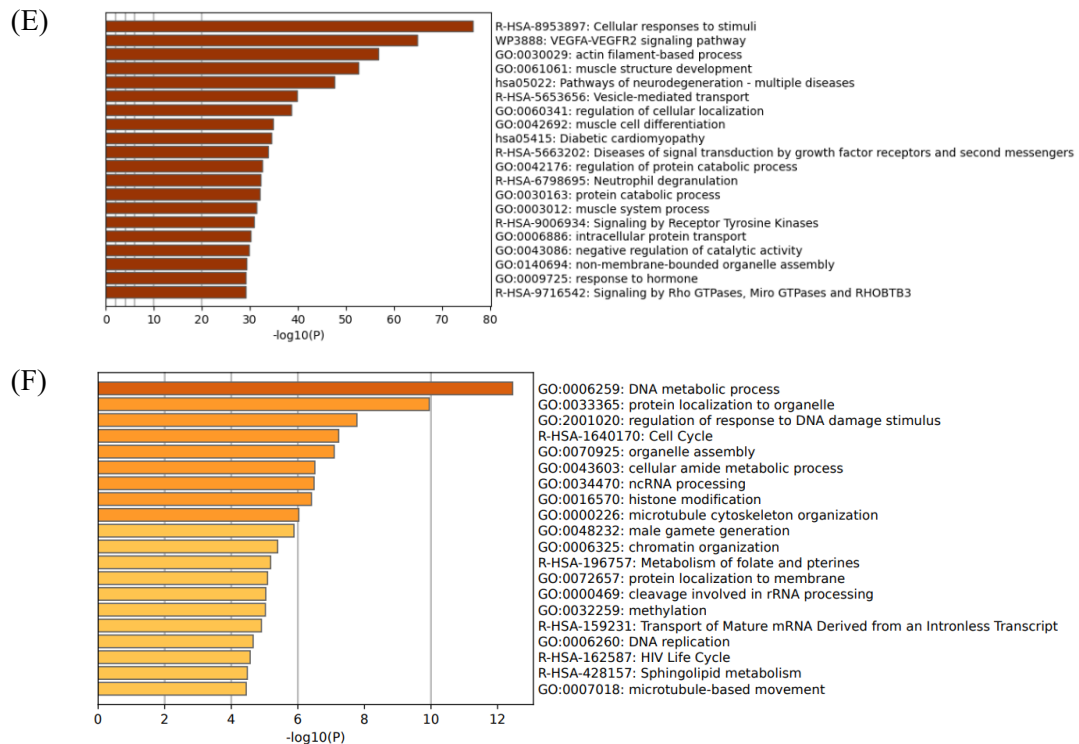


Figure 3. Gene enrichment analysis of DEGs. (A) Gene enrichment analysis of DEGs upregulated in DM. (B) Gene enrichment analysis of DEGs downregulated in DM. (C) Gene enrichment analysis of DEGs upregulated in PM. (D) Gene enrichment analysis of DEGs downregulated in PM. (E) Gene enrichment analysis of DEGs upregulated in dysferlinopathy. (F) Gene enrichment analysis of DEGs downregulated in dysferlinopathy.

Table 3. Upregulated DEGs involved in the interferon alpha/beta signaling pathway (R-HSA-909733) in DM.

Gene symbol	Function reported to be associated with interferon alpha/beta signaling pathway
-------------	---

<i>MX1</i>	IFN1-stimulated gene
<i>MX2</i>	IFN1-stimulated gene
<i>OAS1</i>	IFN1-stimulated gene
<i>OAS2</i>	IFN1-stimulated gene
<i>OAS3</i>	IFN1-stimulated gene
<i>STAT2</i>	Transcription factor of IFN1-stimulated gene
<i>ISG15</i>	IFN1-stimulated gene
<i>IFI6</i>	IFN1-stimulated gene
<i>IFI27</i>	IFN1-stimulated gene
<i>IFI35</i>	IFN1-stimulated gene
<i>IFIT1</i>	IFN1-stimulated gene
<i>IFIT2</i>	IFN1-stimulated gene
<i>IFIT3</i>	IFN1-stimulated gene
<i>IFIT5</i>	IFN1-stimulated gene
<i>IFITM1</i>	IFN1-stimulated gene
<i>IFITM3</i>	IFN1-stimulated gene
<i>IRF1</i>	Transcription factor of IFN1-stimulated gene
<i>HLA-A</i>	MHC-I formation
<i>HLA-B</i>	MHC-I formation
<i>HLA-C</i>	MHC-I formation
<i>PSMB8</i>	Catalytic subunit of immunoproteasomes, which mediates proteolysis and generates MHC-I molecules
<i>SOCS3</i>	Negative IFN1 regulator
<i>USP18</i>	Negative IFN1 regulator
<i>SAMHD1</i>	IFN1-stimulated gene
<i>XAF1</i>	IFN1-stimulated gene
<i>RSAD2</i>	IFN1-stimulated gene

Abbreviations: IFN1, type 1 interferon; MHC-I, major histocompatibility complex class I

Table 4. Upregulated DEGs involved in the antigen processing and presentation of peptide antigen pathway (GO:0048002) in PM.

Gene symbol	Reported function
<i>B2M</i>	Involved in MHC-I peptide-loading complex
<i>CD74</i>	Essential for assembly and stabilization during HLA class II antigen presentation
<i>PDIA3</i>	Involved in MHC-I peptide-loading complex
<i>HLA-C</i>	MHC-I formation
<i>HLA-DRA</i>	MHC-II formation
<i>TAP1</i>	Involved in MHC-I peptide-loading complex
<i>TAPBPL</i>	Binds to MHC-I coupled with beta2-microglobulin
<i>CDKN1A</i>	Regulator of cell cycle progression
<i>GADD45A</i>	Growth arrest and DNA damage-inducible protein
<i>ITGAL</i>	Involved in cellular adhesion and costimulatory signaling
<i>PSMD1</i>	Degradation machinery of intracellular proteolysis
<i>ICAM2</i>	Member of the intercellular adhesion molecule family
<i>KIF22</i>	Involved in spindle formation and chromosome movement during mitosis and meiosis
<i>SPTBN2</i>	Probably plays an important role in the neuronal membrane skeleton
<i>TNFRSF14</i>	Participates in bidirectional cell-cell contact signaling between antigen-presenting cells and lymphocytes
<i>SOCS3</i>	Mediates the ubiquitination and subsequent proteasomal degradation of target proteins
<i>DTX3L</i>	Plays a role in DNA damage repair and IFN-mediated antiviral responses
<i>RHOC</i>	Regulates a signal transduction pathway linking plasma membrane

	receptors to the assembly of focal adhesions and actin stress fibers
<i>ZNF627</i>	May be involved in transcriptional regulation
<i>CREB3L2</i>	Transcription factor involved in unfolded protein response
<i>IFIT3</i>	IFN-induced antiviral protein
<i>PLAU</i>	Specifically cleaves the zymogen plasminogen to form the active enzyme plasmin
<i>GSDMD</i>	Precursor of a pore-forming protein that plays a key role in host defense against pathogen infection and danger signals
<i>TBC1D10C</i>	Inhibits the Ras signaling pathway via its intrinsic Ras GTPase-activating protein activity

Abbreviations: MHC-I, major histocompatibility complex class I; MHC-II, major histocompatibility complex class II; HLA, human leukocyte antigen; IFN, interferon

4. Identification of key modules and genes, using coexpression analysis

In the case of the DEGs upregulated in DM, the PPI network comprised 370 DEGs and 1311 interaction pairs. The MCODE analysis revealed 6 modules, including 71 nodes and 311 pairs. The key module (MCODE score = 11) contained 23 genes related to the interferon alpha/beta signaling pathway (R-HSA-909733), with 253 pairs (Figure 4-A). The 23 genes in this module were closely linked to each other, and the degree score of all these genes was 22. These genes corresponded to DEGs mapped to the IFN1 signaling pathway in the gene enrichment analysis.

In the case of the DEGs downregulated in DM, the PPI network comprised 317 DEGs and 2123 interaction pairs. The MCODE analysis revealed 7 modules, including 78 nodes and 874 pairs. The key module (MCODE score = 19) contained 41 genes related to the eukaryotic translation elongation pathway (R-HSA-156842), with 794 pairs (Figure 4-B). Of the 41 genes, the following 24 genes had the highest degree score of 40: *RPL10A*,

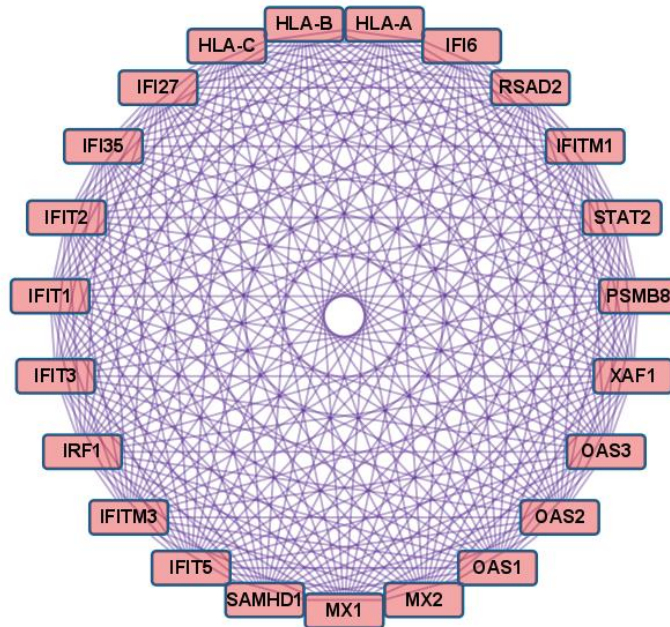
RPL4, RPL7, RPL13, RPL21, RPL26, RPL27, RPL30, RPLP2, RPS3, RPS5, RPS11, RPS13, RPS14, RPS15, RPS15A, RPS16, RPS20, RPS21, RPS23, RPS25, RPS28, RPL35, and RPL13A.

In the case of DEGs upregulated in PM, the PPI network consisted of 59 DEGs and 63 interaction pairs. The MCODE analysis revealed 2 modules, including 7 nodes and 9 pairs. The key module (MCODE score = 1.5) contained 4 genes (*PDIA3, HLA-C, B2M, and TAPI*) related to the antigen processing and presentation pathway (GO:0048002) (Figure 5-A).

In the case of DEGs downregulated in PM, the PPI network consisted of 27 DEGs and 32 interaction pairs. The MCODE analysis results revealed 2 modules, including 8 nodes and 12 pairs. The key module (MCODE score = 1.7) contained 5 genes (*MYBPC2, TNNI2, TNNT3, TNNC2, and MYH1*) related to the striated muscle contraction pathway (R-HSA-390522) (Figure 5-B).

In the case of dysferlinopathy, no network was identified in the PPI analysis of up- or downregulated DEGs.

(A)



(B)

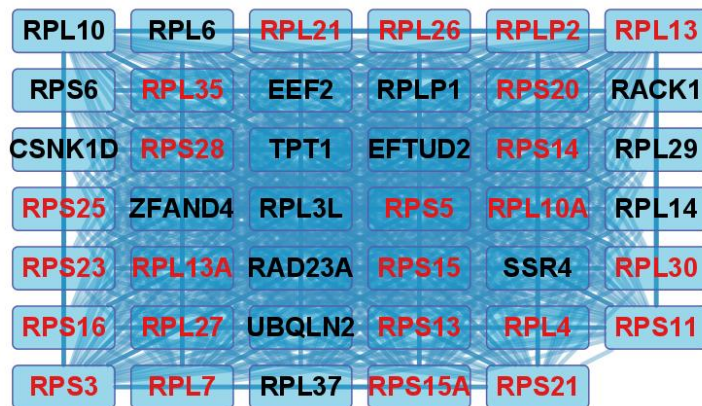
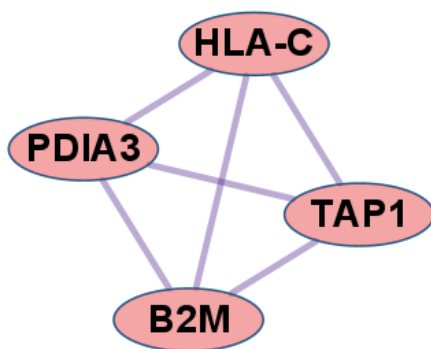


Figure 4. Coexpression analysis of DEGs in DM. (A) MCODE analysis of upregulated DEGs reveals the key module containing 23 genes related to the IFN1 signaling pathway (R-HSA-909733). (B) MCODE analysis of downregulated DEGs reveals the key module

containing 41 genes related to the eukaryotic translation elongation pathway (R-HSA-156842). The 24 genes with the highest degree score of 40 are marked in red.

(A)



(B)

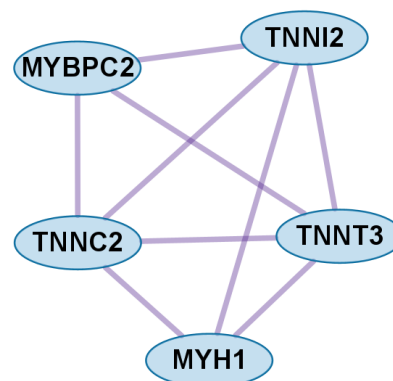


Figure 5. Coexpression analysis of DEGs in PM. (A) MCODE analysis of upregulated DEGs reveals the key module containing 4 genes related to the antigen processing and presentation of peptide antigen pathway (GO:0048002). (B) MCODE analysis of downregulated DEGs reveals the key module containing 5 genes related to the striated muscle contraction pathway (R-HSA-390522).

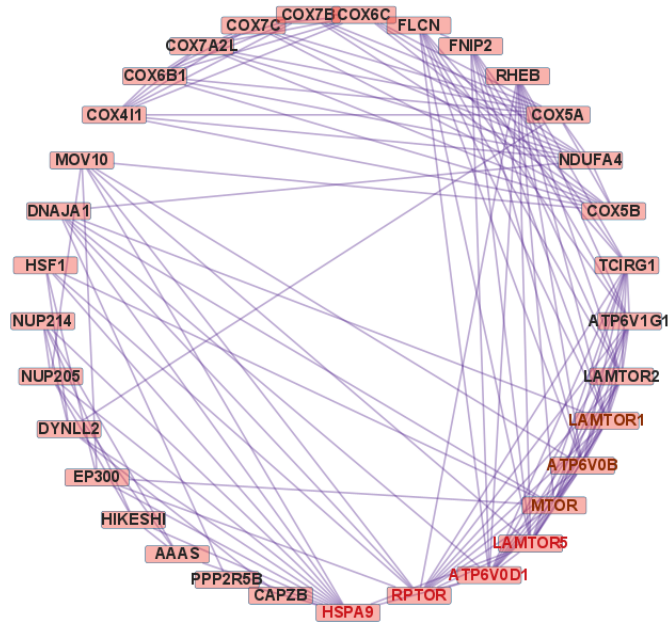
5. Identification of hub genes within important biological pathways in dysferlinopathy

We performed PPI analysis with 261 upregulated DEGs related to the cellular response to stimuli (R-HSA-8953897) to identify hub genes in this pathway. This PPI network comprised 261 DEGs and 5420 interaction pairs. The MCODE analysis revealed 8

modules, including 185 nodes and 2891 pairs. The key module (MCODE score = 4.12) contained 32 genes related to the cellular response to stress (R-HSA-2262752), with 134 pairs. Of the 32 genes, 4 (*HSPA9*, *RPTOR*, *ATP6V0D1*, and *LAMTOR5*) had the highest degree score of 13 and 3 (*MTOR*, *LAMTOR1*, and *ATP6V0B*) had a score of 12 (Figure 6-A).

We performed PPI analysis with 62 downregulated DEGs related to the DNA metabolic process (GO:0006259) to identify hub genes in this pathway. The PPI network comprised 43 DEGs and 117 interaction pairs. The MCODE analysis revealed 3 modules, including 20 nodes and 40 pairs. The key module (MCODE score = 2.63) contained 11 genes (*ATAD5*, *RAD9A*, *RAD17*, *TP53BP1*, *RFC5*, *RFC4*, *MCM9*, *WDR48*, *FAN1*, *EME1*, and *EME2*) related to the cellular response to DNA damage stimulus (GO:0006974), with 29 pairs. Of the 11 genes, *RFC4* was found to have the highest degree score of 8 (Figure 6-B).

(A)



(B)

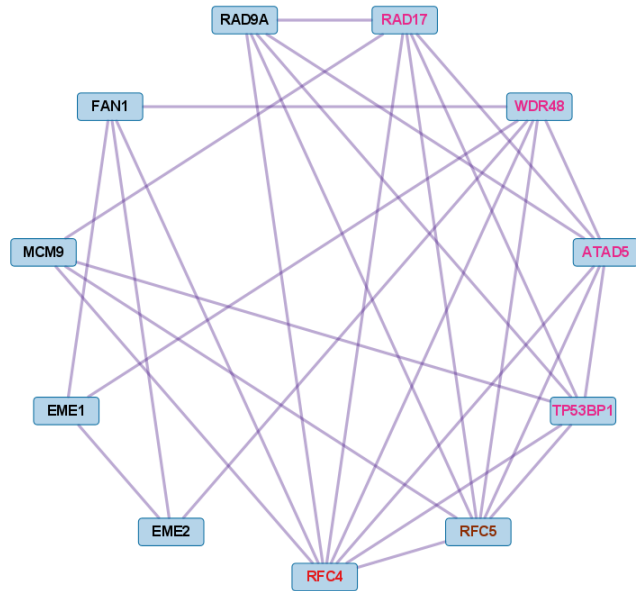
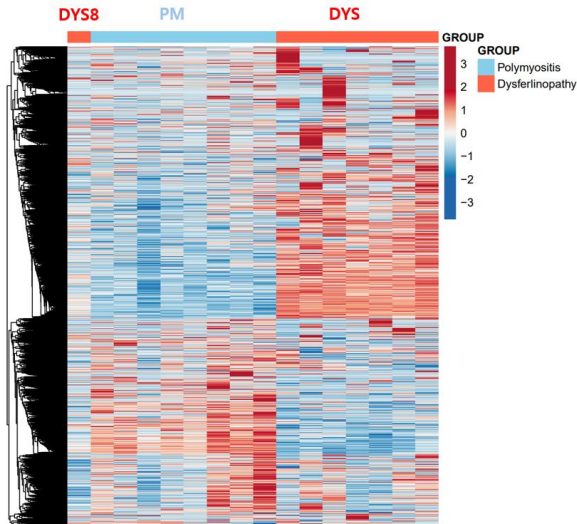


Figure 6. Coexpression analysis of DEGs mapped to important pathways in dysferlinopathy. (A) PPI with 261 upregulated DEGs related to the cellular response to stimuli (R-HSA-8953897). MCODE analysis reveals the key module containing 32 genes related to the cellular response to stress (R-HSA-2262752). The 4 genes with the highest degree score of 13 are marked in red, and the 3 genes with a score of 12 are marked in brown. (B) PPI with 62 downregulated DEGs related to the DNA metabolic process (GO:0006259). MCODE analysis reveals the key module containing 11 genes related to the cellular response to DNA damage stimulus (GO:0006974). The gene with the highest degree score of 8 is marked in red, the gene with a score of 7 in brown, and the 4 genes with a score of 6 in pink.

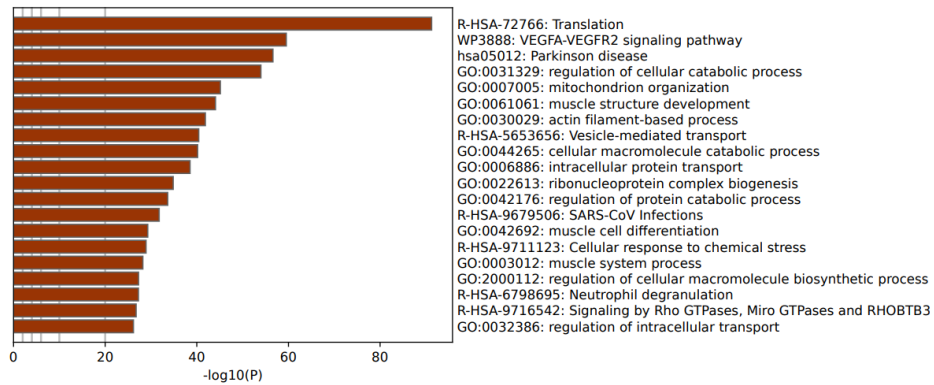
6. Comparative analysis between PM and dysferlinopathy

The results revealed that 2869 DEGs were upregulated in dysferlinopathy and 1444 DEGs in PM (Figure 7-A). PPI analysis of the upregulated DEGs did not identify any networks for dysferlinopathy or PM. Gene enrichment analysis results for the DEGs upregulated in dysferlinopathy and PM have been presented in Figure 7-B and C, respectively. The DEGs upregulated in dysferlinopathy were most abundant in the translation pathway (R-HSA-72766), and 775 DEGs were mapped to this reactome pathway. PPI analysis of the 775 DEGs mapped to the translation pathway (R-HSA-72766) did not identify any network. The DEGs upregulated in PM were most abundant in the protein localization to organelle pathway (GO:0033365), and 58 DEGs were mapped to this GO pathway. PPI analysis of 58 DEGs mapped to the protein localization to organelle pathway (GO:0033365) showed that the network was composed of 35 DEGs and 42 pairs. The MCODE analysis results revealed 1 module, including 4 nodes and 6 pairs (Figure 7-D). These 4 genes (*KDELR3*, *COPB2*, *TMED7*, and *RAB1A*) were related to endoplasmic reticulum (ER) to Golgi vesicle-mediated transport (GO:0006888).

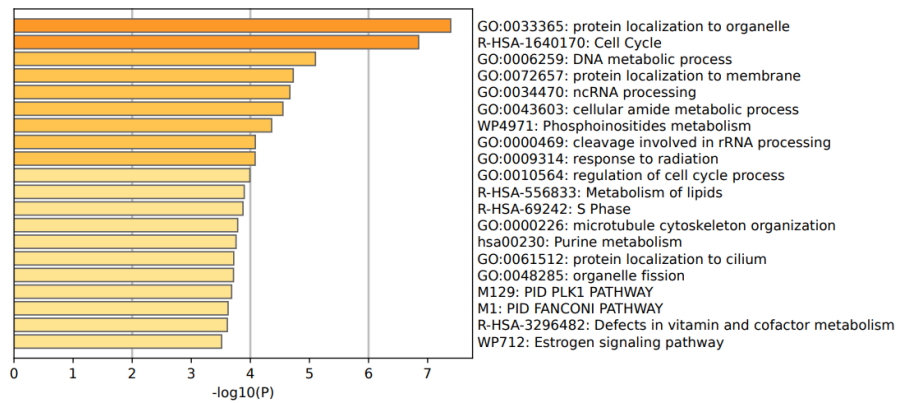
(A)



(B)



(C)



(D)

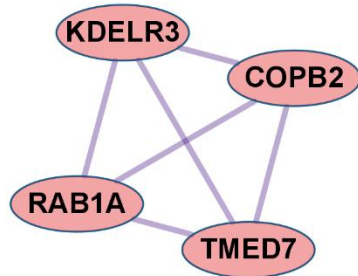


Figure 7. Comparative analysis between PM and dysferlinopathy. (A) Heat map of the genes differentially expressed between PM and dysferlinopathy. (B) Gene enrichment analysis of DEGs upregulated in dysferlinopathy. (C) Gene enrichment analysis of DEGs upregulated in PM. (D) Coexpression analysis of DEGs mapped to the protein localization to organelle pathway (GO:0033365) in PM. MCODE analysis shows 1 module, including 4 genes related to endoplasmic reticulum to Golgi vesicle-mediated transport (GO:0006888).

IV. DISCUSSION

In this study, we performed bioinformatics analysis of the gene expression profiles obtained for the muscles of patients with DM, PM, or dysferlinopathy. Gene enrichment analysis revealed that upregulated DEGs were most abundant in the IFN1 signaling pathway in DM and the antigen processing and presentation of peptide antigen pathway in PM. The DEGs upregulated in dysferlinopathy were most abundant in the cellular response to stimuli.

1. IFN1 signaling pathway in DM

Analysis of muscle transcripts from patients with DM helped identify 26 upregulated DEGs involved in the interferon alpha/beta signaling pathway. Of these, 18 were IFN1-stimulated genes (ISGs), which included 2 ISG transcription factor–encoding genes (*STAT2* and *IRF1*), 2 IFN1 negative regulator–encoding genes (*SOCS3* and *USP18*), and 3 genes involved in MHC-I formation (*HLA-A*, *HLA-B*, and *HLA-C*).

Prominent IFN1 pathway activation occurs in DM, and ISG overexpression has been detected in the peripheral blood, skin, and muscle of patients with DM.^{4,5,8,29-32} IFN1-related proteins are prominent in DM muscles and are considered a potential DM diagnostic biomarker.^{33,34} Additionally, the IFN1 pathway biomarker in blood is highly correlated with clinical severity in DM.³² Analysis of different subgroups for DM muscle biopsies has shown that the IFN1 signature is a useful unifying pattern for all DM subgroups and can be used to differentiate DM from other diseases.³⁵

The ISGs such as *MX*, *ISG15*, *OAS*, *IFITM*, *IFIT*, and *IFI* observed in our results have also been reported as hub genes in a bioinformatics study performed using muscle from a patient with DM.^{30,36,37} Myxovirus resistance protein 1 (MxA) is a key mediator of the interferon-induced antiviral response against a variety of viruses.³⁸ Sarcoplasmic MxA expression has been shown to be a DM hallmark, and the European NeuroMuscular Center (ENMC) 2018 DM classification criteria include perifascicular MxA overexpression as definite DM muscle biopsy findings.³⁵ *ISG15* is one of the most

strongly induced ISGs; it was also found to be selectively overexpressed in muscle from adult patients who had DM with perifascicular atrophy.³⁹ A previous study proposed that the *ISG15* expression level in muscle alone could be used to reliably quantify IFN1 pathway activation in adult inflammatory myositis.⁴⁰ In patients with juvenile DM, muscle *ISG15* expression was found to be inversely correlated with the clinical and histological severity of the disease; these results suggest that *ISG15* negatively regulates the IFN1 signaling pathway.⁴¹ Thus, *ISG15* may be used as a biomarker for DM diagnosis and monitoring; further research on the use of *ISG15* for this purpose is expected. The expression of *USP18* and *SOCS3*, which are negative regulators of IFN1 pathway signaling,⁴¹⁻⁴³ was also found to increase in the current study. The possibility of their involvement in regulating sustained IFN1 signaling pathway activation in DM can be considered. Among the other genes analyzed in this study, *STAT2* and *IRF1* which are ISG transcription factors, have been reported to be overexpressed in DM.²⁹

The mechanisms underlying IFN1 induction in DM remain unclear. IFN1 is secreted from dendritic cells because of Toll-like receptor (TLR) induction and from muscle cells because of retinoic acid-inducible gene 1 (RIG-1) activation.⁴⁴ Direct response by a viral pathogen or secondary response associated with muscle tissue remodeling may cause TLR induction.⁴⁵ *ISG15* and *IFIT3*, which are overexpressed in DM, are upregulated in IFN-mediated antiviral immunity, suggesting possible viral contribution to DM.⁴⁶ An in vitro study showed that hypoxia triggers IFN1 production in muscles.⁴⁷

The IFN1 pathway plays an important role with respect to muscle fibers and vascular injury in DM pathophysiology. In vitro studies have shown that IFN1 impairs myoblast differentiation and endothelial cell angiogenesis and interferes with vascular network organization.^{5,48,49} Autocrine IFN1 signaling was recently found to prevent muscle stem cell proliferation in DM, leading to muscle repair deficit.⁵⁰ These in vitro pathogenic effects of IFN1 in muscle and endothelial cells can be prevented by pharmacologic blockade of IFN1 signaling by using JAK inhibitors or anti-IFN receptor antibodies.^{49,50} A systematic literature review suggested that JAK inhibitors represent a viable treatment

option for DM.⁵¹ For treating cutaneous disease in DM, possible future options include subcutaneous immunoglobulin and JAK kinase inhibitors such as tofacitinib, ruxolitinib, or tocilizumab, all of which are currently under clinical trial.⁵²

2. Antigen processing and presentation of peptide antigen pathway in PM

Analysis of muscle transcripts from patients with PM helped identify 4 upregulated DEGs (*PDIA3*, *TAP1*, *B2M*, and *HLA-C*) involved in antigen processing and peptide antigen presentation. All these genes encode proteins involved in MHC-I formation and quality control. Normal muscle fibers do not express MHC-I, but MHC-I overexpression has been histopathologically confirmed in the muscles of patients with PM or IBM, and the inflammatory response by the MHC-I–CD8 complex is a major pathological mechanism in PM.^{53,54} Thus, our findings are consistent with those of previous studies.

Protein disulfide-isomerase A3 (*PDIA3*), transporter associated with antigen processing 1 (*TAP1*), and beta2-microglobulin (*B2M*) are involved in the MHC-I peptide loading complex (PLC).^{55,56} The PLC, a transient multisubunit membrane complex in the ER, is essential for establishing stable peptide–MHC-I complexes by stringent peptide proofreading and quality control processes.⁵⁶ TAP, a central part of the PLC, ensures high local concentrations of translocated peptides in the ER lumen proximal to the PLC.^{56,57} *PDIA3* acts as a chaperone; it forms a disulfide-linked complex with tapasin as a component of the MHC-I loading complex, which is thought to either stabilize the complex or facilitate correct class I molecule assembly.⁵⁸ The other PLC constituents, namely, calreticulin, tapasin, and ERp57, function in recruiting and stabilizing peptide–MHC-I. These concerted actions ensure that only MHC-I molecules loaded with optimal peptide epitopes are released from the PLC.⁵⁹

3. Cellular response to stress in dysferlinopathy

Analysis of muscle transcripts from patients with dysferlinopathy helped identify the following 7 upregulated DEGs involved in the cellular response to stress: *HSPA9*, *RPTOR*,

MTOR, LAMTOR1, LAMTOR5, ATP6V0D1, and ATP6V0B.

A. *HSPA9*

HSPA9 encodes mortalin, a 74 kDa mitochondrial-resident protein also known as p66mot-1, mitochondrial stress-70 protein (mtHsp70), peptide-binding protein 74 (PBP74), and glucose-regulated protein 75 (GRP75).^{60,61} Mortalin is located in the mitochondria, ER, plasma membrane, cytoplasmic vesicles, and cytosol.⁶² Its activity and function are determined by its cellular localization and binding partners.⁶⁰ Many studies have shown that mortalin has a variety of functions; it has been found to play both protective and destructive roles in various cell types. Mortalin overexpression provides an important line of defense against accumulated proteins, inflammation, and neuronal loss.⁶³ It is enriched in several types of cancer and contributes to carcinogenesis in various ways.⁶⁴

GRP75 (mortalin) levels in human skeletal muscles increase with oxidative stress occurring during high- or low-intensity training or during disuse.^{65,66} GRP75 expression has been found to increase in the muscles of patients with inflammatory myositis. GRP75 levels were found to increase in nonregenerating myofibers of patients who had myositis and were positive for sarcolemmal MHC-I immunoreactivity; the increase in GRP75 immunoreactivity involved both mitochondria and glycolytic fibers.⁶⁷ GRP75 is also involved in mediating endo/sarcoplasmic reticulum (ER/SR)–mitochondria Ca^{2+} transport by forming the inositol 1,4,5-triphosphate receptor (IP3R)–GRP75–voltage-dependent anion channel 1 (VDAC1) complex in skeletal muscle cells.⁶⁸ Changes in ER/SR-mitochondria Ca^{2+} transport may be related to impaired skeletal muscle function, such as in Duchenne muscular dystrophy (DMD),⁶⁹ or age-related muscle dystrophy.⁷⁰ Dysferlin is involved in T-tubule biogenesis and Ca^{2+} homeostasis maintenance.⁷¹⁻⁷³ *HSPA9* overexpression may be related to changes in intramuscular Ca^{2+} homeostasis. *HSPA9* has varying functions depending on the cell type and interacting proteins; therefore, further research is required to clarify the significance of intramuscular *HSPA9*

expression in dysferlinopathy.

B. Mammalian target of rapamycin complex 1 (mTORC1) pathway

Regulatory-associated protein of MTOR complex 1 (RPTOR; *RPTOR*), *MTOR*, and late endosomal/lysosomal adaptor, MAPK, and MTOR activator (*LAMTOR*) are associated with the mTOR pathway. The mTORC1 is composed of regulatory associated protein of mTOR (raptor), proline-rich Akt substrate of 40 kDa (PRAS40), DEP domain-containing mTOR-interacting protein (DEPTOR), and mammalian lethal with SEC13 protein 8 (mLST8).⁷⁴ mTORC1 signaling is a key regulator of skeletal muscle mass.⁷⁵ mTORC1 also acts as an upstream regulator of autophagy induction in skeletal muscle.⁷⁶ Chronic mTORC1 activation in old muscle leads to muscle atrophy mainly because of inability to induce autophagy.⁷⁷ Autophagy dysregulation is related to various hereditary myopathies, including autophagic vacuolar myopathies.⁷⁶ Autophagy was found to be impaired in patients with DMD and in mdx mouse models. In mdx mice, mTOR was constitutively activated, leading to autophagy-inducing gene downregulation at the molecular level.⁷⁸ In dysferlinopathy, the autophagy program has been found to be activated for degradation of mutant dysferlin aggregates.¹⁷ Inhibition of mutant dysferlin aggregate formation in the ER by rapamycin, an mTOR inhibitor, has been reported in a cellular model.⁷⁹ A recently published bioinformatics analysis involving dysferlinopathy identified the genes involved in the ubiquitin–proteasome pathway as key genes.⁸⁰ Thus, our results suggest that the mTORC1 and autophagy pathways play a role in dysferlinopathy pathogenesis.

4. DEGs downregulated in DM, PM, and dysferlinopathy

Gene enrichment analysis revealed that downregulated DEGs were most abundant in eukaryotic translation elongation in DM and striated muscle contraction in PM. The DEGs downregulated in dysferlinopathy were most abundant in the DNA metabolic process.

Twenty-four ribosome-associated genes were found to be downregulated on analyzing muscle transcripts from patients with DM. Decreased ribosomal-associated gene expression has recently been detected in the muscle and skin in juvenile DM.⁸¹ Analysis of muscle transcripts from patients with PM helped identify 5 downregulated DEGs (*MYBPC2*, *TNNI2*, *TNNT3*, *TNNC2*, and *MYH1*) related to striated muscle contraction. These findings may reflect muscle degeneration in DM and PM.

Analysis of muscle transcripts from patients with dysferlinopathy identified 6 downregulated DEGs (*RFC4*, *RFC5*, *ATAD5*, *TP53BP1*, *WDR48*, and *RAD17*) related to the cellular response to DNA damage stimulus. Replication factor C (RFC) plays an important role in DNA replication and repair, cell proliferation, cell cycle checkpoint regulation, and cell growth under stress.⁸² However, the implications of reduced RFC expression in dysferlinopathy require further study because association between myopathy and RFC expression has not been reported.

5. Comparative analysis between PM and dysferlinopathy

Comparative analysis between PM and dysferlinopathy revealed that the DEGs upregulated in PM were most abundant in the protein localization to organelle pathway and helped identify 4 genes (*KDELR3*, *COPB2*, *TMED7*, and *RAB1A*) that were related to ER to Golgi vesicle-mediated transport. However, no promising pathway or gene that could be used as a biomarker for differentiating PM from dysferlinopathy was identified.

6. Limitations of this study

This study has several limitations. First, myositis-specific antibodies were not tested in patients with DM or PM. In particular, while interpreting the PM results, it should be noted that the gene expression patterns in PM were not clearly differentiated from those of the control. PM is reported to be an overdiagnosed entity as subgroups of inflammatory myopathy are subdivided. A diagnosis of PM should be considered only after excluding the other disease subgroups. Therefore, confirmation with a complete myositis

autoantibody panel, especially including the anti-3-hydroxy-3-methylglutaryl coenzyme A reductase (HMGCR) antibody, is recommended for differentiation from immune-mediated necrotizing myositis.⁸³ However, we could not perform this confirmatory analysis because we did not have serum samples from the patients. Second, 1 patient with dysferlinopathy (DYS8) showed a different gene expression pattern among the dysferlinopathy groups. This result was consistent with the pathological findings for dysferlin expression. Dysferlin expression was completely lost in the other patients; however, only this patient (DYS8) showed reduced expression. For the interpretation of this results, it would be helpful to collect additional dysferlinopathy cases in which the dysferlin was expressed and analyze the intramuscular transcriptome profiles of these patients. Third, the sample size of the dataset used in this study was small; therefore, the results obtained from the bioinformatics analysis should be further verified. Fourth, several of the hub genes identified in this study have not been previously reported to be associated with dysferlinopathy; therefore, further *in vitro* and functional studies are required to verify the molecular biological mechanisms of the genes identified in this study.

V. CONCLUSION

In conclusion, we identified differential biological pathways on the basis of bioinformatics analysis of gene expression profiles obtained from the muscles of patients with DM, PM, or dysferlinopathy. Overexpression of genes related to the IFN1 signaling pathway was identified in DM, and overexpression of genes related to MHC-I formation and quality control was identified in PM. In dysferlinopathy, overexpression of *HSPA9* and the mTORC1 signaling pathway genes was detected. Further studies are required to verify the role of *HSPA9* and the mTORC1 pathway in the pathomechanism of dysferlinopathy.

REFERENCES

1. Schmidt J. Current Classification and Management of Inflammatory Myopathies. *J Neuromuscul Dis* 2018;5:109-29.
2. Gao S, Luo H, Zhang H, Zuo X, Wang L, Zhu H. Using multi-omics methods to understand dermatomyositis/polymyositis. *Autoimmun Rev* 2017;16:1044-8.
3. Zhou X, Dimachkie MM, Xiong M, Tan FK, Arnett FC. cDNA microarrays reveal distinct gene expression clusters in idiopathic inflammatory myopathies. *Med Sci Monit* 2004;10:Br191-7.
4. Suárez-Calvet X, Gallardo E, Nogales-Gadea G, Querol L, Navas M, Díaz-Manera J, et al. Altered RIG-I/DDX58-mediated innate immunity in dermatomyositis. *J Pathol* 2014;233:258-68.
5. Greenberg SA, Pinkus JL, Pinkus GS, Burleson T, Sanoudou D, Tawil R, et al. Interferon-alpha/beta-mediated innate immune mechanisms in dermatomyositis. *Ann Neurol* 2005;57:664-78.
6. Baechler EC, Bauer JW, Slattery CA, Ortmann WA, Espe KJ, Novitzke J, et al. An interferon signature in the peripheral blood of dermatomyositis patients is associated with disease activity. *Mol Med* 2007;13:59-68.
7. Walsh RJ, Kong SW, Yao Y, Jallal B, Kiener PA, Pinkus JL, et al. Type I interferon-inducible gene expression in blood is present and reflects disease activity in dermatomyositis and polymyositis. *Arthritis Rheum* 2007;56:3784-92.
8. Wong D, Kea B, Pesich R, Higgs BW, Zhu W, Brown P, et al. Interferon and biologic signatures in dermatomyositis skin: specificity and heterogeneity across diseases. *PLoS One* 2012;7:e29161.
9. Venalis P, Lundberg IE. Immune mechanisms in polymyositis and dermatomyositis and potential targets for therapy. *Rheumatology (Oxford)* 2014;53:397-405.
10. Amato AA, Brown RH, Jr. Dysferlinopathies. *Handb Clin Neurol* 2011;101:111-8.
11. Han R, Campbell KP. Dysferlin and muscle membrane repair. *Curr Opin Cell Biol* 2007;19:409-16.

12. Klinge L, Laval S, Keers S, Haldane F, Straub V, Barresi R, et al. From T-tubule to sarcolemma: damage-induced dysferlin translocation in early myogenesis. *FASEB J* 2007;21:1768-76.
13. Sharma A, Yu C, Leung C, Trane A, Lau M, UtoKaparch S, et al. A new role for the muscle repair protein dysferlin in endothelial cell adhesion and angiogenesis. *Arterioscler Thromb Vasc Biol* 2010;30:2196-204.
14. Han R. Muscle membrane repair and inflammatory attack in dysferlinopathy. *Skelet Muscle* 2011;1:10.
15. Mariano A, Henning A, Han R. Dysferlin-deficient muscular dystrophy and innate immune activation. *FEBS J* 2013;280:4165-76.
16. Han R, Frett EM, Levy JR, Rader EP, Lueck JD, Bansal D, et al. Genetic ablation of complement C3 attenuates muscle pathology in dysferlin-deficient mice. *J Clin Invest* 2010;120:4366-74.
17. Fanin M, Nascimbeni AC, Angelini C. Muscle atrophy, ubiquitin-proteasome, and autophagic pathways in dysferlinopathy. *Muscle Nerve* 2014;50:340-7.
18. Roche JA, Tulapurkar ME, Mueller AL, van Rooijen N, Hasday JD, Lovering RM, et al. Myofiber damage precedes macrophage infiltration after in vivo injury in dysferlin-deficient A/J mouse skeletal muscle. *Am J Pathol* 2015;185:1686-98.
19. Trapnell C, Roberts A, Goff L, Pertea G, Kim D, Kelley DR, et al. Differential gene and transcript expression analysis of RNA-seq experiments with TopHat and cufflinks. *Nat Protoc* 2012;7:562-78.
20. Ji F, Sadreyev RI. RNA-seq: Basic Bioinformatics Analysis. *Curr Protoc Mol Biol* 2018;124:e68.
21. Lundberg IE, Tjärnlund A, Bottai M, Werth VP, Pilkington C, de Visser M, et al. 2017 European League Against Rheumatism/American College of Rheumatology Classification Criteria for Adult and Juvenile Idiopathic Inflammatory Myopathies and Their Major Subgroups. *Arthritis Rheumatol* 2017;69:2271-82.
22. Dobin A, Davis CA, Schlesinger F, Drenkow J, Zaleski C, Jha S, et al. STAR:

- ultrafast universal RNA-seq aligner. *Bioinformatics* 2013;29:15-21.
23. Ashburner M, Ball CA, Blake JA, Botstein D, Butler H, Cherry JM, et al. Gene ontology: tool for the unification of biology. The Gene Ontology Consortium. *Nat Genet* 2000;25:25-9.
 24. Kanehisa M, Goto S. KEGG: kyoto encyclopedia of genes and genomes. *Nucleic Acids Res* 2000;28:27-30.
 25. Fabregat A, Jupe S, Matthews L, Sidiropoulos K, Gillespie M, Garapati P, et al. The Reactome Pathway Knowledgebase. *Nucleic Acids Res* 2018;46:D649-d55.
 26. Zhou Y, Zhou B, Pache L, Chang M, Khodabakhshi AH, Tanaseichuk O, et al. Metascape provides a biologist-oriented resource for the analysis of systems-level datasets. *Nat Commun* 2019;10:1523.
 27. Shannon P, Markiel A, Ozier O, Baliga NS, Wang JT, Ramage D, et al. Cytoscape: a software environment for integrated models of biomolecular interaction networks. *Genome Res* 2003;13:2498-504.
 28. Bader GD, Hogue CW. An automated method for finding molecular complexes in large protein interaction networks. *BMC Bioinformatics* 2003;4:2.
 29. Kuriyama Y, Shimizu A, Kanai S, Oikawa D, Motegi SI, Tokunaga F, et al. Coordination of retrotransposons and type I interferon with distinct interferon pathways in dermatomyositis, systemic lupus erythematosus and autoimmune blistering disease. *Sci Rep* 2021;11:23146.
 30. Xiao L, Xiao W, Lin S. Ten genes are considered as potential biomarkers for the diagnosis of dermatomyositis. *PLoS One* 2021;16:e0260511.
 31. Tanboon J, Nishino I. Update on dermatomyositis. *Curr Opin Neurol* 2022; doi:10.1097/wco.0000000000001091.
 32. Huard C, Gullà SV, Bennett DV, Coyle AJ, Vleugels RA, Greenberg SA. Correlation of cutaneous disease activity with type 1 interferon gene signature and interferon β in dermatomyositis. *Br J Dermatol* 2017;176:1224-30.
 33. Suárez-Calvet X, Gallardo E, Pinal-Fernandez I, De Luna N, Lleixà C, Díaz-

- Manera J, et al. RIG-I expression in perifascicular myofibers is a reliable biomarker of dermatomyositis. *Arthritis Res Ther* 2017;19:174.
34. Uruha A, Nishikawa A, Tsuburaya RS, Hamanaka K, Kuwana M, Watanabe Y, et al. Sarcoplasmic MxA expression: A valuable marker of dermatomyositis. *Neurology* 2017;88:493-500.
 35. Mammen AL, Allenbach Y, Stenzel W, Benveniste O. 239th ENMC International Workshop: Classification of dermatomyositis, Amsterdam, the Netherlands, 14-16 December 2018. *Neuromuscul Disord* 2020;30:70-92.
 36. Chen S, Li H, Zhan H, Zeng X, Yuan H, Li Y. Identification of hub biomarkers and immune cell infiltration in polymyositis and dermatomyositis. *Aging (Albany NY)* 2022;14:4530-55.
 37. Ouyang X, Zeng Y, Jiang X, Xu H, Ning Y. Identification of Vital Hub Genes and Potential Molecular Pathways of Dermatomyositis by Bioinformatics Analysis. *Biomed Res Int* 2021;2021:9991726.
 38. Haller O, Kochs G. Human MxA protein: an interferon-induced dynamin-like GTPase with broad antiviral activity. *J Interferon Cytokine Res* 2011;31:79-87.
 39. Salajegheh M, Kong SW, Pinkus JL, Walsh RJ, Liao A, Nazareno R, et al. Interferon-stimulated gene 15 (ISG15) conjugates proteins in dermatomyositis muscle with perifascicular atrophy. *Ann Neurol* 2010;67:53-63.
 40. Pinal-Fernandez I, Casal-Dominguez M, Derfoul A, Pak K, Plotz P, Miller FW, et al. Identification of distinctive interferon gene signatures in different types of myositis. *Neurology* 2019;93:e1193-e204.
 41. Hou C, Durrleman C, Periou B, Barnerias C, Bodemer C, Desguerre I, et al. From Diagnosis to Prognosis: Revisiting the Meaning of Muscle ISG15 Overexpression in Juvenile Inflammatory Myopathies. *Arthritis Rheumatol* 2021;73:1044-52.
 42. Carow B, Rottenberg ME. SOCS3, a Major Regulator of Infection and Inflammation. *Front Immunol* 2014;5:58.
 43. Zhao L, Wang Q, Zhou B, Zhang L, Zhu H. The Role of Immune Cells in the

- Pathogenesis of Idiopathic Inflammatory Myopathies. *Aging Dis* 2021;12:247-60.
44. Bolko L, Jiang W, Tawara N, Landon-Cardinal O, Anquetil C, Benveniste O, et al. The role of interferons type I, II and III in myositis: A review. *Brain Pathol* 2021;31:e12955.
 45. Cappelletti C, Baggi F, Zolezzi F, Biancolini D, Beretta O, Severa M, et al. Type I interferon and Toll-like receptor expression characterizes inflammatory myopathies. *Neurology* 2011;76:2079-88.
 46. Baechler EC, Bilgic H, Reed AM. Type I interferon pathway in adult and juvenile dermatomyositis. *Arthritis Res Ther* 2011;13:249.
 47. De Luna N, Suárez-Calvet X, Lleixà C, Diaz-Manera J, Olivé M, Illa I, et al. Hypoxia triggers IFN-I production in muscle: Implications in dermatomyositis. *Sci Rep* 2017;7:8595.
 48. Franzì S, Salajegheh M, Nazareno R, Greenberg SA. Type 1 interferons inhibit myotube formation independently of upregulation of interferon-stimulated gene 15. *PLoS One* 2013;8:e65362.
 49. Ladislau L, Suárez-Calvet X, Toquet S, Landon-Cardinal O, Amelin D, Depp M, et al. JAK inhibitor improves type I interferon induced damage: proof of concept in dermatomyositis. *Brain* 2018;141:1609-21.
 50. Gally L, Fermon C, Lessard L, Weiss-Gayet M, Viel S, Streichenberger N, et al. Involvement of Type I Interferon Signaling in Muscle Stem Cell Proliferation During Dermatomyositis. *Neurology* 2022;98:e2108-e19.
 51. Paik JJ, Lubin G, Gromatzky A, Mudd PN, Jr., Ponda MP, Christopher-Stine L. Use of Janus kinase inhibitors in dermatomyositis: a systematic literature review. *Clin Exp Rheumatol* 2022; doi:10.55563/clinexprheumatol/hxin60.
 52. Wright NA, Vleugels RA, Callen JP. Cutaneous dermatomyositis in the era of biologicals. *Semin Immunopathol* 2016;38:113-21.
 53. Ikenaga C, Kubota A, Kadoya M, Taira K, Uchio N, Hida A, et al. Clinicopathologic features of myositis patients with CD8-MHC-1 complex

- pathology. *Neurology* 2017;89:1060-8.
54. Dalakas MC. Inflammatory muscle diseases. *N Engl J Med* 2015;372:1734-47.
 55. Margulies DH, Jiang J, Natarajan K. Structural and dynamic studies of TAPBPR and Tapasin reveal the mechanism of peptide loading of MHC-I molecules. *Curr Opin Immunol* 2020;64:71-9.
 56. Blees A, Janulienė D, Hofmann T, Koller N, Schmidt C, Trowitzsch S, et al. Structure of the human MHC-I peptide-loading complex. *Nature* 2017;551:525-8.
 57. Neefjes J, Jongstra ML, Paul P, Bakke O. Towards a systems understanding of MHC class I and MHC class II antigen presentation. *Nat Rev Immunol* 2011;11:823-36.
 58. Mahmood F, Xu R, Awan MUN, Song Y, Han Q, Xia X, et al. PDIA3: Structure, functions and its potential role in viral infections. *Biomed Pharmacother* 2021;143:112110.
 59. Domnick A, Winter C, Sušac L, Hennecke L, Hensen M, Zitzmann N, et al. Molecular basis of MHC I quality control in the peptide loading complex. *Nat Commun* 2022;13:4701.
 60. Londono C, Osorio C, Gama V, Alzate O. Mortalin, apoptosis, and neurodegeneration. *Biomolecules* 2012;2:143-64.
 61. Kaul SC, Taira K, Pereira-Smith OM, Wadhwa R. Mortalin: present and prospective. *Exp Gerontol* 2002;37:1157-64.
 62. Wadhwa R, Taira K, Kaul SC. An Hsp70 family chaperone, mortalin/mthsp70/PBP74/Grp75: what, when, and where? *Cell Stress Chaperones* 2002;7:309-16.
 63. Priyanka, Seth P. Insights Into the Role of Mortalin in Alzheimer's Disease, Parkinson's Disease, and HIV-1-Associated Neurocognitive Disorders. *Front Cell Dev Biol* 2022;10:903031.
 64. Yoon AR, Wadhwa R, Kaul SC, Yun CO. Why is Mortalin a Potential Therapeutic Target for Cancer? *Front Cell Dev Biol* 2022;10:914540.

65. Gjøvaag TF, Dahl HA. Effect of training and detraining on the expression of heat shock proteins in m. triceps brachii of untrained males and females. *Eur J Appl Physiol* 2006;98:310-22.
66. Dalla Libera L, Ravara B, Gobbo V, Tarricone E, Vitadello M, Biolo G, et al. A transient antioxidant stress response accompanies the onset of disuse atrophy in human skeletal muscle. *J Appl Physiol* (1985) 2009;107:549-57.
67. Vitadello M, Doria A, Tarricone E, Ghirardello A, Gorza L. Myofiber stress-response in myositis: parallel investigations on patients and experimental animal models of muscle regeneration and systemic inflammation. *Arthritis Res Ther* 2010;12:R52.
68. Zhang SS, Zhou S, Crowley-McHattan ZJ, Wang RY, Li JP. A Review of the Role of Endo/Sarcoplasmic Reticulum-Mitochondria Ca(2+) Transport in Diseases and Skeletal Muscle Function. *Int J Environ Res Public Health* 2021;18.
69. Pauly M, Angebault-Prouteau C, Dridi H, Notarnicola C, Scheuermann V, Lacampagne A, et al. ER stress disturbs SR/ER-mitochondria Ca(2+) transfer: Implications in Duchenne muscular dystrophy. *Biochim Biophys Acta Mol Basis Dis* 2017;1863:2229-39.
70. Del Campo A, Contreras-Hernández I, Castro-Sepúlveda M, Campos CA, Figueroa R, Tevy MF, et al. Muscle function decline and mitochondria changes in middle age precede sarcopenia in mice. *Aging (Albany NY)* 2018;10:34-55.
71. Kerr JP, Ward CW, Bloch RJ. Dysferlin at transverse tubules regulates Ca(2+) homeostasis in skeletal muscle. *Front Physiol* 2014;5:89.
72. Hofhuis J, Bersch K, Büssenschütt R, Drzymalski M, Liebetanz D, Nikolaev VO, et al. Dysferlin mediates membrane tubulation and links T-tubule biogenesis to muscular dystrophy. *J Cell Sci* 2017;130:841-52.
73. Hofhuis J, Bersch K, Wagner S, Molina C, Fakuade FE, Iyer LM, et al. Dysferlin links excitation-contraction coupling to structure and maintenance of the cardiac transverse-axial tubule system. *Europace* 2020;22:1119-31.

74. Wullschleger S, Loewith R, Hall MN. TOR signaling in growth and metabolism. *Cell* 2006;124:471-84.
75. Yoon MS. mTOR as a Key Regulator in Maintaining Skeletal Muscle Mass. *Front Physiol* 2017;8:788.
76. Xia Q, Huang X, Huang J, Zheng Y, March ME, Li J, et al. The Role of Autophagy in Skeletal Muscle Diseases. *Front Physiol* 2021;12:638983.
77. Castets P, Lin S, Rion N, Di Fulvio S, Romanino K, Guridi M, et al. Sustained activation of mTORC1 in skeletal muscle inhibits constitutive and starvation-induced autophagy and causes a severe, late-onset myopathy. *Cell Metab* 2013;17:731-44.
78. De Palma C, Morisi F, Cheli S, Pambianco S, Cappello V, Vezzoli M, et al. Autophagy as a new therapeutic target in Duchenne muscular dystrophy. *Cell Death Dis* 2012;3:e418.
79. Fujita E, Kouroku Y, Isoai A, Kumagai H, Misutani A, Matsuda C, et al. Two endoplasmic reticulum-associated degradation (ERAD) systems for the novel variant of the mutant dysferlin: ubiquitin/proteasome ERAD(I) and autophagy/lysosome ERAD(II). *Hum Mol Genet* 2007;16:618-29.
80. Xie Y, Li YH, Chen K, Zhu CY, Bai JY, Xiao F, et al. Key biomarkers and latent pathways of dysferlinopathy: Bioinformatics analysis and in vivo validation. *Front Neurol* 2022;13:998251.
81. Roberson EDO, Mesa RA, Morgan GA, Cao L, Marin W, Pachman LM. Transcriptomes of peripheral blood mononuclear cells from juvenile dermatomyositis patients show elevated inflammation even when clinically inactive. *Sci Rep* 2022;12:275.
82. Li Y, Gan S, Ren L, Yuan L, Liu J, Wang W, et al. Multifaceted regulation and functions of replication factor C family in human cancers. *Am J Cancer Res* 2018;8:1343-55.
83. Loarce-Martos J, Lilleker JB, Parker M, McHugh N, Chinoy H. Polymyositis: is

there anything left? A retrospective diagnostic review from a tertiary myositis centre. *Rheumatology (Oxford)* 2021;60:3398-403.

ABSTRACT(IN KOREAN)

생물정보학 접근법을 이용한 피부근염, 다발근염, 디스펠린근육병에서
골격근의 상대적인 전사체 분석

<지도교수 최 영 철>

연세대학교 대학원 의학과

정 하 늘

연구배경: 피부근염과 다발근염은 특발성 염증성 근육병의 구분되는 질환이다. 디스펠린근육병은 디스펠린 유전자 돌연변이에 의해 발생하며 일반적으로 청소년기 후반에 근력 약화를 보이게 된다. 퇴행성 근육 변화는 종종 염증 침윤을 동반하여 다발근염으로 오진하기도 한다.

연구목적: 생물정보학 접근법을 이용하여 피부근염, 다발근염 및 디스펠린근육병과 관련된 주요 생물학적 경로 및 유전자를 식별함으로써 각 질환의 병리를 이해하고 치료 개발을 위한 지침을 얻고자 한다.

연구방법: 피부근염 환자 7명, 다발근염 환자 8명, 디스펠린근육병 환자 8명, 대조군 5명의 가쪽넓은근육 생검 조직에 대해 리보핵산 시퀀싱(sequencing)을 수행하였다. 각 환자군에서 차별적으로 발현된 유전자는 DESeq2를 사용하여 확인하였다. 차별적으로 발현된 유전자들의 기능과 관여하는 생물학적 경로를 확인하기 위해 증폭 분석(enrichment analysis)을 수행하였다. 네트워크 분석을 위해서 단백질-단백질 상호작용 방법을 이용하였고, 질병과 관련된 주요 유전자를 확인하기 위해 molecular complex detection tool (MCODE)를 사용하였다.

연구결과: 피부근염, 다발근염, 디스펠린근육병에서 각각 총 1048, 179, 3807개의 차별적으로 발현된 유전자가 발견되었다. 유전자 증폭 분석을 통해 각 질환에서 발현이 증가한 유전자들이 관련된 생물학적 경로를 확인하였다. 피부근염에서는 1형 인터페론 신호전달 경로, 다발근염에서는 항원 처리 및 펩타이드 항원 제시, 디스펠린근육병에서는 자극에 대한 세포반응이 주요 생물학적 경로임을 확인하였다. 단백질-단백질 상호작용 및 MCODE

알고리즘을 이용한 네트워크 분석 결과 각 질환에서 발현이 증가한 주요 유전자들을 확인하였다. 피부근염에서는 1형 인터페론 신호전달 경로와 관련한 23개의 유전자(*IFI6, IFI27, IFI35, IFIT1, IFIT2, IFIT3, IFIT5, IFITM1, IFITM3, IRF1, MX1, MX2, OAS1, OAS2, OAS3, HLA-A, HLA-B, HLA-C, STAT2, PSMB8, SAMHD1, XAF1, and RSAD2*), 다발근염에서는 1형 주조직 적합성 복합체 (MHC class I)의 형성과 조절에 관여하는 4개의 유전자(*PDIA3, HLA-C, B2M, and TAP1*), 디스펠린근육병에서는 스트레스에 대한 세포 반응에 관여하는 7개의 유전자(*HSPA9, RPTOR, MTOR, LAMTOR1, LAMTOR5, ATP6V0D1, and ATP6V0B*) 가 주요 유전자로 발견되었다.

결론: 생물정보학 접근법을 이용한 근육내 전사체 분석 연구를 통해 피부근염에서 1형 인터페론 신호 전달과 관련한 유전자의 과발현과 다발근염에서 1형 주조직 적합성 복합체와 관련한 유전자들의 과발현을 확인하였다. 디스펠린근육병에서는 *HSPA9* 및 mammalian target of rapamycin complex 1(mTORC1) 신호 전달과 관련한 유전자들을 발견하였다. 본 연구 결과는 병인 및 치료에 대한 향후 연구에 새로운 방향을 제시할 수 있다.

핵심되는 말 : 피부근염, 다발근염, 디스펠린근육병, 전사체 분석, 리보핵산 시퀀싱, 생물정보학 분석